Article

Differential Expression of Proteins in Response to Ceramide-Mediated Stress Signal in Colon Cancer Cells by 2-D Gel Electrophoresis and MALDI-TOF–MS

M. Fillet, C. Cren-Oliv, A.-F. Renert, J. Piette, F. Vandermoere, Ch. Rolando, and M-P. Merville

J. Proteome Res., **2005**, 4 (3), 870-880 • DOI: 10.1021/pr050006t

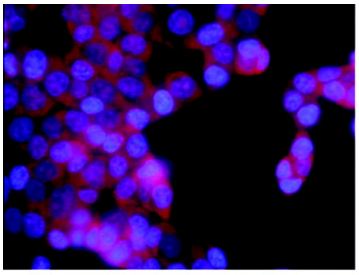

Untreated cells

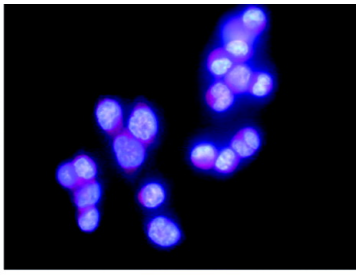

Cells treated with C6-ceramide

research articles Journal of proteome research

Differential Expression of Proteins in Response to Ceramide-Mediated Stress Signal in Colon Cancer Cells by 2-D Gel Electrophoresis and MALDI-TOF−MS

M. Fillet,*,† C. Cren-Olivé,‡ A.-F. Renert,† J. Piette,† F. Vandermoere,§ Ch. Rolando,‡ and M-P. Merville†

Laboratories of Clinical Chemistry and Virology, Center for Biomedical Integrated Genoproteomic, University of Liège, Sart-Tilman, Belgium, and CNRS UMR8009, University of Sciences and Technologies of Lille, 59650 Villeneuve d'Ascq, France, and UPRES-EA 1033, INSERM-ESPRI, IFR-118 Proteomics, University of Sciences and Technologies of Lille, 59650 Villeneuve d'Ascq, France

Received January 19, 2005

Comparative cancer cell proteome analysis is a strategy to study the implication of ceramides in the transmission of stress signals. To better understand the mechanisms by which ceramide regulate some physiological or pathological events and the response to the pharmacological treatment of cancer, we performed a differential analysis of the proteome of HCT-116 (human colon carcinoma) cells in response to these substances. We first established the first 2-dimensional map of the HCT-116 proteome. Then, HCT116 cell proteome treated or not with C6-ceramide have been compared using two-dimensional electrophoresis, matrix-assisted laser desorption/ionization-mass spectrometry and bioinformatic (genomic databases). 2-DE gel analysis revealed more than fourty proteins that were differentially expressed in control cells and cells treated with ceramide. Among them, we confirmed the differential expression of proteins involved in apoptosis and cell adhesion.

Keywords: 2-D gel • MALDI-TOF−MS • cancer cells • ceramide

Introduction

For many years, sphingolipids have been regarded as structural inert components of cell membranes. The relevance of sphingolipids as intracellular modulators emerged with the observation made by Okazaki and co-workers that sphingomyelin hydrolysis and ceramide generation could be triggered by diverse stimuli in a wide variety of cell types.[1] Since then, many studies have demonstrated the crucial role played by ceramide in the development of human diseases, including ischaemia/reperfusion injury, insulin resistance and diabetes, atherogenesis, septic shock, and ovarian failure. Furthermore, ceramide signaling mediates the therapeutic effects of chemotherapy and radiotherapy in some cells.[2] An understanding of the mechanisms by which ceramide regulates physiological and pathological events in specific cells may provide new targets for pharmacological intervention.

The sphingomyelin pathway is an ubiquitous signaling system that links specific cell-surface receptors and physical stress to the nucleus. Recent data demonstrate that ceramide play an important role in one or several stages of apoptosis. Indeed, several cytokines and environment stress known to initiate apoptosis, including Tumor Necrosis Factor-α (TNF-α), CD95/Fas/APO-1, chemotherapeutic drugs, ionizing and ultraviolet radiation, heat shock and oxidative stress appear to induce a rapid rise of intracellular ceramide concentration.[3−7] The clarification of the role of ceramide may provide further insights into the treatment of several human diseases such as cancer.

Several studies showed that exogenous cell-permeable ceramide analogues reproduced many of the biological effects of these agents, suggesting a role for the generated ceramide in mediating and regulating cell responses.[8,9] To gain additional insights into the mechanisms governing cell stress mediated by ceramide, we used a systematic approach to study the pattern of proteins whose expression varies upon ceramide treatment of HCT-116 cancer cells (human colon carcinoma). One commonly used is two-dimensional electrophoresis (2-DE), which is a highly resolving technique for arraying proteins by isoelectric point and molecular mass. When immobilized pH gradients (IPGs) are used for isoelectric focusing in the first dimension, excellent reproducibility and high protein load capacity can be achieved.[10] Using Coomassie bleue staining, protein spots on the gel can be visualized and differences in protein levels determined using appropriate 2-D analysis software. Digested proteins of interest can then be identified by MALDI-TOF mass spectrometry. This combination of tech-

* To whom correspondence should be addressed. M. Fillet, Laboratory of Clinical Chemistry, CHU B23, University of Liège, Sart-Tilman, 4000 Liège, Belgium. Tel.: 0032-4-3662472. Fax: 0032-4-3664534. E-mail address: marianne.fillet@ulg.ac.be.

† Laboratories of Clinical Chemistry and Virology, Center for Biomedical Integrated Genoproteomic, University of Liège.

‡ CNRS UMR8009, University of Sciences and Technologies of Lille.

§ UPRES-EA 1033, INSERM-ESPRI, IFR-118 Proteomics, University of Sciences and Technologies of Lille.

10.1021/pr050006t CCC: $30.25
Published on Web 05/07/2005

niques makes possible to study a profile of changes in protein levels.

Studies can be facilitated by comparing the gels obtained with 2-DE reference gels representing the typical pattern of the cells studied under normal conditions. To the best of our knowledge, detailed 2-DE reference map of HCT116 cells is not currently available to the scientific community. This is why we first started with the HCT116 cells reference map and then compared it with gels made of HCT116 cells treated with C6-ceramide.

The association of two-dimensional electrophoresis with matrix-assisted laser desorption/ionization time-of-flight mass spectrometry and database interrogations allowed us to identify 43 proteins differentially expressed in HCT116 cells after C6-ceramide treatment. Beside cytoskeletal proteins such as actin, tubulin and tropomyosin, we identified various proteins more especially implicated in regulation of apoptosis, protein synthesis, metabolic activity, growth, cell mobility and also components of RNA-processing pathways confirming the crucial role of ceramide in cellular homeostasis. This approach provided new insights into the proteins involved in response to the stress signals mediated by ceramide.

Materials and Methods

Cell Culture and Biological Reagents. The HCT116 cell line is derived from a human colorectal carcinoma and has been used as a model for colon cancer. HCT-116 human colon carcinoma cells (ATCC CCL 247) were cultured in McCoy's 5A modified medium (Life Technologies, Inc.) supplemented with 10% fetal bovine serum, 1% L-glutamine (200 mM), 100 units/ml penicillin and 100 μg/mL streptomycin. The cells were maintained at 37 °C in a 5% CO_2 atmosphere.

C6-ceramide was obtained from Sanver Tech (Boechout, Belgium) and was solubilized in ethanol.

Protein Extraction. HCT116 cells were washed three times with ice-cold PBS. Cells were lysed with a buffer containing 50 mM Tris pH 7.5, 100 mM NaCl, 5 mM EDTA, 0.1% (v/v) Triton $\times$100, 7M urea, 4% (v/v) CHAPS, 65 mM DTT, protease-inhibitors (Complete kit, Roche Diagnostics, Germany) during 30 min at −20 °C. Cellular debris were removed by centrifugation for 15 min at 20 000 $\times$ *g* and at 4 °C. Total proteins were precipitated with ethanol and solubilized in a sample solution containing 7 M urea, 2 M thiourea, 4% CHAPS, 0.04 M Tris base, 65 mM DTT.

Proteins samples were stored at −20 °C until the protein amounts was quantified using the commercial kit from Amersham Biosciences PlusOne 2-D Quant Kit (Uppsala, Sweden). In some cases, HCT116 cells were treated with 50 μM C6-ceramide during 6 h.

Two-Dimensional Gel Electrophoresis. Proteins samples (400 μg of total proteins) were mixed with 225 μL of loading buffer for IPG strips (Genomic Solutions) and 225 μL of urea solubilization/rehydratation buffer for IPG strips (Genomic Solutions) to obtain a final volume of 450 μL. The mixture was applied in gel for reswelling with a dry immobilized pH gradient (IPG) 180 mm, pH 3−10 linear gradient (Immobiline DryStrip, Amersham Pharmacia Biotech) on a Ettan IPGphor system (Amersham Pharmacia). Complete sample uptake into the strips was achieved after 9 h at 20 °C with a voltage of 50 V. Focusing was performed at 200 V for 1 h at 1000 V for 1 h, and at 8000 V for 13 h. Current was limited to 50 μA per strip, and temperature maintained at 20 °C for all IEF steps. For SDS-PAGE, the IPG strips were incubated in equilibration buffer containing 37.5 mM Tris-HCL (pH 8.8), 6 M urea, 2% (w/vol) SDS, 30% (vol/vol) glycerol, and 2% (w/vol) DTT for 15 min, and then incubated for 15 min in equilibration buffer supplemented with 2.5% (w/vol) iodoacetamide. The equilibrated IPG strips were transferred for the second dimension (SDS-PAGE) onto 10% Duracryl (Genomic solutions, Steinheim, Germany) gels (255 $\times$ 205 $\times$ 1.5 mm). Electrophoresis was carried out at 20 °C using a Ettan Daltsix system (Amersham Pharmacia) with 25 mM Tris as the running buffer, 192 mM glycine containing 0.1% w/vol SDS, at 15 mA per gel for 16 h, until the bromophenol blue had reached the bottom of the gel.

Data are means of three independent experiments. For the differentiel analysis, statistical significance was estimated with Student's *t*-test. A p value of < 0.05 was considered significant.

Staining of 2-DE Gels. Coomassie Bleue staining was performed according to Neuhoff et al.[11] Gels were fixed overnight in 50% vol/vol ethanol containing 2% w/vol orthophosphoric acid. Gels were then incubated for 1 h in 34% vol/vol methanol containing 17% ammonium sulfate, 2% w/vol orthophosphoric acid and 1 g of Coomassie Blue G-250 and then stained with the same solution for 3 days.

2-D Image Analysis. Stained-2D gels were digitalized at 200 dpi resolution using an Imagescanner scanner (Amersham Pharmacia Biotech). A calibration filter using different shades of gray was applied to transform pixel intensities into optical density units. The scans were exported in TIF format and imported into Progenesis V2003−01 2-DE gel image analysis software (Nonlinear Dynamics) for analysis. Briefly, after automatic spot detection, the background was removed from each gel and the images were edited manually, e.g., adding, splitting, and removing spots. One gel was chosen as the master gel, and used for the automatic matching of spots in the other 2-DE gels.

In-Gel Trypsin Digestion. To identify the protein spots, preparative 2-DE gels were excised, cut into 1−2 mm^2 gel pieces and destained at room temperature in 50 mM NH_4HCO_3 buffer pH 8.8 containing 50% acetonitrile (ACN) for 1 to 2 h. After washing with 50 μL ACN, the gel pieces were dehydrated and dried thoroughly in a vacuum centrifuge (Concentrator 5301, Eppendorf, Hamburg, Germany) for a few minutes. The dried gel pieces were rehydrated with 20 μL of 50 mM NH_4HCO_3, pH 8 containing 20 μg/mL trypsin (Promega, Madison, WI) allowing protein digestion at 37 °C overnight. The samples were then dried in a vacuum centrifuge, and resuspended in 10 μL of water before MALDI-MS analysis.

MALDI-TOF−MS and Database Search. For acquisition of the mass spectrometric peptide maps of the proteins, 1 μL of the generated cleavage products was mixed with 1 μL of DHB matrix solution (10 mg dihydrobenzoic acid in 50% methanol/50% water) on the MALDI target. The mixture was air-dried at room temperature prior to the acquisition of the mass spectra. MALDI-TOF−MS was performed using a Voyager DE STR mass spectrometer (PerSeptive Biosystems, Framingham, MA) equipped with a 337.1 nm nitrogen laser and with the delayed extraction facility. All spectra were acquired in a positive ion reflector mode. Typically, 200 laser shots were recorded per sample, and the spectra were internally calibrated (using the DataExplorerTM software, PerSeptive Biosystems, Framingham, MA) using three peptides arising from trypsin autoproteolysis ($[M+H]^+$ 842,5100; $[M+H]^+$ 1045.5642; $[M+H]^+$ 2211.1046). Tryptic monoisotopic peptide masses were searched for in the NCBI, using Mascot software (http://www.matrixscience.com) with a mass tolerance setting of 50 ppm, with one missed

cleavage site as fixed parameters, and with carbamidomethylation and methionine oxidation as variable modifications.

Western Blot Analysis. Total protein extracts were prepared as previously described.[12] Protein amounts were quantified with the micro BCA Protein Assay Reagent kit (Pierce, Rockford).

Analysis of caspase 10 cleavage was assessed by Western Blot analysis. Briefly, 20 μg of protein extracts were run on 10% SDS-PAGE gels, transferred, and incubated with an anti-caspase 10 specific polyclonal antibody (Calbiochem) (1:500), followed by a goat anti-rabbit-specific antibody (1:10000)(Amersham) and developed using enhanced chemiluminescent detection methods (ECL Kit, Amersham Pharmacia Biotech, UK). Analysis of Annexin V was performed with an anti-annexin V polyclonal antibody (1/500) (Santa Cruz). Vascular cell adhesion molecule (VCAM) protein detection was performed with an anti-VCAM polyclonal antibody (1/500) (Santa Cruz). Analysis of PCNA was performed with an anti-PCNA polyclonal antibody (1/200) (Santa Cruz). Finally, caspase 8 protein detection was realized with an anti-caspase 8 polyclonal antibody (1/1000) (BD Pharmigen, CA).

Fluorescent Microscopy. The percentage of apoptotic or necrotic cells was determined by fluorescent microscopy. Cells were fixed with paraformaldehyde, incubated for 15 min. with propidium iodide and DAPI (4′, 6-diamidine-2′-phenylindole dihydrochloride), and then visualized under fluorescent microscopy. The percent of blue cells nuclei (DAPI stained DNA) with apoptotic morphology (nuclear and cytoplasmic condensation, nuclear fragmentation, membrane blebbing, and apoptotic body formation) was determined by examining more than 400 cells per dish. Necrotic cells were characterized by their cytoplasmic staining (propidium iodide stained RNA).

Results

2-DE Pattern of HCT-116 Cells. We first studied the pattern of protein expression in HCT116 cells. A 2-DE map of this cell type was constructed to establish of a 2-DE protein map as a prerequisite for subsequent comparative proteomic studies of ceramide treated cells. For this purpose, total cell extracts were prepared (with a buffer made of urea, CHAPS and DTT) and loaded on 2-DE gels. In the initial isoelectric focusing, samples were applied to IPG strips by incubating the proteins dissolved in rehydratation solution with the strips (active rehydratation). The 2-DE gel system employed was IEF on 180 mm IPG strips (pH 3−10) in the first dimension and 10% SDS-PAGE in the second dimension. After electrophoresis, the gels were stained with Coomassie Blue, and the most visible spots were excised and processed for mass spectrometric analysis. The corresponding proteins were identified by peptide mass fingerprinting and computer analysis (Table 1). Figure 1 represents a comprehensive view of the major proteins expressed in this colon cancer cell. Overall, protein spots were well-resolved, but some vertical streaks persisted even with ethanol precipitation of the protein samples.

More than 1000 spots were detected on the map using the Progenesis software and 120 of them have been identified (Figure 1, Table 1). The results of protein identification are summarized in Table 1, in which we mention the main known/postulated function of the identified proteins.

At least three spots were identified as proteins from the cytoskeleton and/or highly implicated in cell mobility and cellular morphological changes related to angiogenesis (e.g., actin, tubulin and tropomyosin, which typically constitute the framework of the cytoskeletal machinery). The multifunctional proteins Rho GDP dissociation inhibitor, heat shock protein 27, high mobility group protein 2 (HMG 2) and annexin V are ubiquitous and highly regulated proteins which tightly cooperate in actin/tubulin dynamics and/or membrane trafficking.[12−16]

The typical metabolic capabilities of HCT-116 cells were illustrated by the identification of several enzymes, i.e., glutathione-S-transferase P (pGST), thioredoxin peroxidase, protein disulfide isomerases (PDI), inorganic pyrophosphatase, hypoxanthine-guanine phosphorobosyltransferase, glyceraldehyde 3-phosphate dehydrogenase, malate dehydrogenase, phosphoglycerate mutase 1, L-lactate dehydrogenase and nucleoside diphosphate kinase A.

Further studies will be necessary to complete the proteomic analysis of this cellular model by the use of narrow range IPG strips that could increase the number of identified proteins. The 2-DE pattern obtained is characterized by a typical high acidic protein content, and share some similarities with other patterns from various eukaryotic cellular models such as, for example, colorectal epithelial cells or colorectal adenocarcinoma cell line (DL-1) (http://www.expasy.org/ch2d/2d-index.html).

Differential Proteome Analysis of HCT-116 Treated or Not with C6-Ceramide. The next step was the identification of proteins whose expression varied with the stimulation of HCT-116 cells by addition of an exogenous ceramide (C6-ceramide at 50 μM during 6h). In a previous paper,[12] we have shown that the cell viability decreased in a dose- and time-dependent manner after C6-ceramide treatment. In HCT116, a treatment with 50 μM of C6-ceramide during 24h led to fifty percent mortality. In our proteomic study, we decided to choose HCT116 with C6-ceramide at the same concentration (50 μM) during 6h in order to study the target proteins dependent on ceramide stress signal.

As shown in red in Figure 1 and in bold in Table 1, 43 proteins were found to be differentially expressed For three of them a close-up image is presented (Figure 1C−E, corresponding respectively to spot 22: stress induced phosphoprotein, spot 119: proteasome subunit α type 1 and spot 26: caspase 10).

In this study, we found a lower expression of 14−3−3 sigma protein in ceramide treated cells. This protein belongs to a family of highly conserved and abundant proteins. They exist in multiple isoforms and have been implicated as key regulators of various cellular processes such as signal transduction, cell cycle control, apoptosis, stress response and malignant transformation.[17,18]

Moreover, proteins implied in RNA processing were found to be regulated by ceramide treatment. For example, proteins involved in transcription (SET protein, nuclear autoantigen Sp-100), in pre-mRNA splicing (heterogeneous nuclear ribonucleoproteins A2/B1), in nuclear export (heterogeneous nuclear ribonucleoproteins A1), in translation (eukaryotic translation initiation factor 4H, eukaryotic translation initiation factor 6, translationally controlled tumor protein) and in ribosomal activity (heterogeneous nuclear ribonucleoproteins C1/C2, 60S acidic ribosomal protein P0, nucleophosmin) were found to be modulated by ceramide treatment. These data suggest that ceramide could play a role in mRNA maturation and export.

Several proteins involved in glycolytic pathway seem to be regulated by C6-ceramide. Some of them are down-regulated (phosphoserine aminotransferase, inorganic pyrophosphatase), others are upregulated (L-lactate dehydrogenase A chain, aspartate aminotransferase).

Three heat shock proteins such as HSP 27, HSP 90β, and HSP 70/HSP 90-organizing protein were all down-regulated in

Table 1. List of Identified Proteins on HCT116 2-DE Gels

spot	accession no.*	protein name	functions	localization	Mr theor. (Da)	p*I* theor.	sequence coverage (%)	peptide match	normalized delta volum[b]
1	P14625	Endoplasmin precursor (94 kDa glucose-regulated protein) (GRP94)	Molecular chaperone	Endoplasmic reticulum lumen	92470	4.8	43	50	
2	P08238	**Heat shock protein HSP 90-β (HSP 84) (HSP 90)**[c]	Molecular chaperone	Cytoplasmic	83265	5.0	59	49	**−2.0**
3	P19320	**Vascular cell adhesion protein 1 precursor (V−CAM 1)**	Cell−cell recognition	Membrane protein	82322	5.1	58	13	**2.0**
4	P27797	Calreticulin precursor (CRP55) (Calregulin) (HACBP) (ERp60)	Molecular chaperone	Endoplasmic reticulum lumen	48142	4.3	61	27	
5	P13667	Protein disulfide isomerase A4 precursor (Protein ERp-72) (ERp72)	Catalytic activity	Endoplasmic reticulum lumen	72933	5.0	45	20	
6	P11142	Heat shock cognate 71 kDa protein	Chaperone		70899	5.4	55	36	
7	P50990	T-complex protein 1, theta subunit (TCP-1-theta) (CCT-theta)	Molecular chaperone	Cytoplasmic	59621	5.4	38	24	
8	P15311	Ezrin (p81) (Cytovillin) (Villin 2)	Component of the microvilli of intestinal epithelial cells	Cytoskeleton	69399	5.9	52	51	
9							46	40	
10	P05218	**Tubulin β-5 chain**	Cytoskeleton	Nuclear	49671	4.8	50	28	**3.8**
11	P06576	ATP synthase β chain, mitochondrial precursor	Catalytic activity	Mitochondrial	56560	5.3	50	28	
12							40	18	
13	P10809	60 kDa heat shock protein, mitochondrial precursor (Hsp60)	Mitochondrial protein import and macromolecular assembly	Mitochondrial	61055	5.7	65	45	
14	P50502	Hsc70-interacting protein (Hip)	Chaperone activity	Cytoplasmic	41332	5.2	51	28	
15	P14868	*Aspartyl-tRNA synthetase*	Catalytic activity	Cytoplasmic	57137	6.1	51	23	**−5.5**
16	P31930	Ubiquinol-cytochrome C reductase complex core protein I, mitochondrial precursor	Catalytic activity	Mitochondrial inner membrane	52619	5.9	53	24	
17	P30101	Protein disulfide isomerase A3 precursor	Catalytic activity	Endoplasmic reticulum lumen	56783	6.0	90	60	
18							74	43	
19	P49368	T-complex protein 1, γ subunit	Molecular chaperone	Cytoplasmic	60403	6.1	46	34	
20	P40227	T-complex protein 1, ζ subunit (TCP-1-ζ)	Molecular chaperone	Cytoplasmic	58025	6.2	41	28	
21	P02545	Lamin A/C (70 kDa lamin)	Cytoskeleton	Nuclear	74140	6.6	58	40	
22	P31948	**Stress-induced-phosphoprotein 1 (STI1) (Hsp70/Hsp90-organizing protein)**	Mediates the association of the molecular chaperones HSC70 and HSP90	Nuclear and cytoplasmic	62640	6.4	55	46	**−2.3**
23	Q03252	Lamin B2	Cytoskeleton	Nuclear	67689	5.3	44	32	
24	Q14790	**Caspase-8**	Apoptosis	Cytoplasmic	55391	5.0	65	17	**1.5**
25	P78371	T-complex protein 1, β subunit (TCP-1-β) (CCT-β)	Molecular chaperone	Cytoplasmic	57489	6.0	60	34	
26	Q92851	**Caspase-10**	Apoptosis		59601	6.9	33	12	**8.1**
27	P12268	Inosine-5′-monophosphate dehydrogenase 2	Catalytic activity		55805	6.4	44	28	

Table 1. (Continued)

spot	accession no.*	protein name	functions	localization	Mr theor. (Da)	p*I* theor.	sequence coverage (%)	peptide match	normalized delta volum[b]
28	Q92804	TATA-binding protein associated factor 2N (RNA-binding protein 56) (TAFII68) (TAF(II)68)	RNA and ssDNA-binding protein	Nuclear	61830	8.0	57	31	
29	*P*23497	**Nuclear autoantigen Sp-100**	Control gene expression	Nuclear	103405	8.5	39	8	**2.1**
30	P52272	Heterogeneous nuclear ribonucleoprotein M (hnRNP M)	Pre-mRNA binding proteins	Nuclear	77470	8.9	57	39	
31							40	35	
32	P30086	Phosphatidylethanolamine-binding protein	Binds ATP	Cytoplasmic	21057	7.0	62	12	
33	P06748	**Nucleophormism (NPM) (Nucleolar phosphoprotein B23)**	Assembly and transport of ribosome	Nuclear	32575	4.6	53	20	**7.9**
34							39	20	
35							35	15	
36	P02570	**Actin, cytoplasmic 1 (*β*-actin)**	Cell mobility	Cytoplasmic	41737	5.3	69	20	**−2.0**
37	P02571	Actin, cytoplasmic 2 (*γ*-actin)	Cell mobility	Cytoplasmic	41793	5.3	70	33	
38	P12277	Creatine kinase, B chain (B−CK)	Catalytic activity	Cytoplasmic	42645	5.3	64	50	
39	P11413	Glucose-6-phosphate 1-dehydrogenase (G6PD)	Catalytic activity		59266	6.4	67	17	
40	P48637	**Glutathione synthetase (GSH−S)**	Protection against oxidative damage	Cytoplasmic	53620	5.1	43	16	**−4.8**
41	P26641	Elongation factor 1-*γ* (EF-1-*γ*) (eEF-1B *γ*)	Anchor		50119	6.3	47	31	
42	P50395	Rab GDP dissociation inhibitor *β* (Rab GDI *β*) (GDI-2)	Regulates the GDP/GTP exchange reaction		50664	6.1	43	24	
43	Q09160	HLA class I histocompatibility antigen, A-80 α chain	Presentation of foreign antigens to the immune system	Type I membrane protein	40792	5.9	66	21	
44	P49411	**Elongation factor Tu, (EF-Tu) mitochondrial precursor**	Protein biosynthesis	Mitochondrial	49542	7.3	81	46	**2.0**
45	P06733	α enolase (Enolase 1)	Catalytic activity glycolysis	Cytoplasmic	47169	7.0	71	40	
46	O43865	Putative adenosylhomocysteinase 2 (S-adenosyl-L-homocysteine hydrolase) (AdoHcyase)	Catalytic activity		55628	7.8	50	12	
47	O00232	26S proteasome non-ATPase regulatory subunit 12 (26S proteasome regulatory subunit p55)	Regulatory subunit of the 26S proteasome		52905	7.5	43	12	
48	O15297	**Protein phosphatase 2C *δ* isoform (p53-induced protein phosphatase 1)**	Growth control		66675	9.1	41	15	**−5.7**
49	P04720	Elongation factor 1-α 1 (EF-Tu)	Protein biosynthesis	Cytoplasmic	50141	9.1	23	13	
50	Q07021	Complement component 1, (Glycoprotein gC1qBP) (p32) (p33)		Mitochondrial	31363	4.7	67	12	
52	P12004	**Proliferating cell nuclear antigen (PCNA) (Cyclin)**	Control of eukaryotic DNA replication	Nuclear	28769	4.6	46	15	**−2.0**
53	P08758	**Annexin A5 (Annexin** V) (Lipocortin V)	Anticoagulant protein		35937	4.9	73	29	**4.5**
54	P42655	14−3−3 protein epsilon (Protein kinase C inhibitor protein-1)	Molecular chaperon	Cytoplasmic	29174	4.6	69	25	
55							37	14	

Table 1. (Continued)

spot	accession no.*	protein name	functions	localization	Mr theor. (Da)	p*I* theor.	sequence coverage (%)	peptide match	normalized delta volum[b]
56	P07910	**Heterogeneous nuclear ribonucleoproteins C1/C2 (hnRNP C1/hnRNP C2)**	Ribonucleosome assembly	Nuclear	33688	5.0	58	13	**3.0**
57	P05209	Tubulin α-1 chain (α-tubulin 1)	Major constituent of microtubules	Nuclear	50152	4.9	59	32	
58	Q9Y265	RuvB-like 1 (49-kDa TATA box-binding)	Transcription	Nuclear	50228	6.0	26	15	
59	P07195	L-lactate dehydrogenase B chain (LDH−B)	Catalytic activity	Cytoplasmic	36639	5.7	63	30	
60			glycolysis				29	15	
61	P12429	Annexin A3 (Annexin III) (Lipocortin III) (Placental anticoagulant protein III)	Inhibitor of phospholipase A2		36376	5.6	47	20	
62	P52788	Spermine synthase (SPMSY)	Catalytic activity		41269	4.9	62	17	
63	Q9UQ80	Proliferation-associated protein 2G4 (Cell cycle protein p38−2G4 homolog) (hG4−1)	Peptidase	Nuclear	43787	6.1	49	23	
64	P17174	**Aspartate aminotransferase, cytoplasmic (Transaminase A)**	Catalytic activity	Cytoplasmic	46116	6.6	45	22	**2.0**
65	P47210	**26S protease regulatory subunit 8 (Proteasome subunit p45)**	Protease	Cytoplasmic	45626	7.1	77	33	**−2.9**
66	Q15365	Poly(rC)-binding protein 1 (α-CP1) (hnRNP-E1) (Nucleic acid binding protein SUB2.3)	Single-stranded nucleic acid binding protein that binds preferentially to oligo dC.	Nuclear	37525	6.7	38	10	
67	Q08752	**40 kDa peptidyl-prolyl *cis*−trans isomerase (PPIase) (Rotamase)**	Proteins folding	Cytoplasmic	40763	6.8	51	19	**−2.0**
68	P04083	Annexin A1 (Annexin I) (Lipocortin I) (P35) (Phospholipase A2 inhibitory protein)	Regulates phospholipase A2 activity		38715	6.6	65	23	
69	Q9Y617	**Phosphoserine aminotransferase (PSAT)**	Catalytic activity	Cytoplasmic	40422	7. 6	44	21	**−2.0**
70	P08865	**40S ribosomal protein SA (P40) (34/67 kDa laminin receptor) (Colon carcinoma laminin-binding protein) (Multidrug resistance-associated protein MGr1-Ag)**	Receptor	Cytoplasmic	32854	4.8	67	19	**−2.1**
71	P48739	Phosphatidylinositol transfer protein *β* isoform	Catalyzes the transfer of PtdIns and phosphatidylcholine between membranes	Cytoplasmic	31540	6.4	61		
72	P25388	**Guanine nucleotide-binding protein *β* subunit-like protein 12.3 (RACK1) (Receptor for activated C kinase)**	Intracellular receptor to anchor the activated PKC to the cytoskeleton		35076	7.6	66	22	**2.6**
73	P36551	**Coproporphyrinogen III oxidase, coproporphirinogenase (COX)**	Catalytic activity	Mitochondrial	40303	6.7	68	24	**−2.0**
74	Q92524	26S protease regulatory subunit S10B (Proteasome subunit p42) (p44)	ATP-dependent degradation of ubiquitinated proteins	Cytoplasmic and nuclear	44173	7.1	70	20	
75	P31947	**14−3−3 protein sigma**	P53-regulated inhibitor of G2/M progression	Cytoplasmic	27774	4.7	54	16	**−2.8**
76	P29312	14−3−3 protein *ζ*/*δ*	Multifunctional regulator of the cell signaling	Cytoplasmic	27745	4.7	50	21	

Table 1. (Continued)

spot	accession no.*	protein name	functions	localization	Mr theor. (Da)	p*I* theor.	sequence coverage (%)	peptide match	normalized delta volum[b]
77	P31946	14−3−3 protein β/α	Multifunctional regulator of the cell signaling	Cytoplasmic	28083	4.8	53	17	
78	P13693	**Translationally controlled tumor protein (TCTP) (p23) (Histamine-releasing factor) (HRF)**	Molecular chaperone	Cytoplasmic	19596	4.8	52	15	**−2.0**
79	P52565	**Rho GDP-dissociation inhibitor 1 (Rho GDI 1)**	Cell mobility	Cytoplasmic	23207	5.0	48	15	**3.8**
80	O00299	**Chloride intracellular channel protein 1**	Chloride ion channel	Nuclear membrane	26923	5.1	48	12	**2.0**
81	P06753	**Tropomyosin α 3 chain**	Binding to actin filament	Cytoplasmic	32818	4.7	80	37	**−3.1**
82	P29692	**Elongation factor 1-*δ* (EF-1-*δ*)**	Protein synthesis		31122	4.9	62	16	**2.0**
83	Q15181	**Inorganic pyrophosphatase (PPase) (Pyrophosphate phospho-hydrolase)**	Catalytic activity	Cytoplasmic	32660	5.5	66	25	**−2.2**
84	Q9Y3B8	Oligoribonuclease, mitochondrial precursor	Role for cellular nucleotide recycling	Mitochondrial	26861	6.4	42	10	
85	P04792	**Heat shock 27 kDa protein (HSP 27) (Stress-responsive protein 27) (SRP27)**	Involved in stress resistance and actin organization	Cytoplasmic Nuclear	22783	6.0	51	13	**−3.1**
86	Q01105	**SET protein (Phosphatase 2A inhibitor I2PP2A)**	Regulation of transcriptional activity	Nuclear	32103	4.1	42	13	**8.2**
87	P05388	**60S acidic ribosomal protein P0 (L10E)**	Ribosomal activity		34273	5.7	53	15	**5.5**
88	P25785	Proteasome subunit α type 1 (proteasome component C2)	Inactivate metalloproteinases	Cytoplasmic	29556	6.1	50	16	
89	P07355	Annexin A2 (Annexin II) (Lipocortin II) (Calpactin I heavy chain)	Calcium-regulated membrane binding protein	Membrane	38604	7.6	58	25	
90							56	23	
91	P00558	Phosphoglycerate kinase 1 (PRP 2)	Catalytic activity		44728	8.3	49	31	
92	P50454	**Collagen-binding protein 2 precursor**	Chaperone	Cytoplasmic	46441	8.7	48	17	**−3.7**
93	Q9UK11	Zinc finger protein 223	Transcription factor	Nuclear	55960	8.9	72	36	
94	P35637	RNA-binding protein FUS (Oncogene FUS) (Oncogene TLS)	Catalytic activity	Nuclear	53426	9.4	39	20	
95	O75947	ATP synthase D chain	Catalytic activity	Mitochondrial	18491	5.2	71	17	
96	P56537	**Eukaryotic translation initiation factor 6 (eIF-6)**	Protein biosynthesis	Cytoplasmic/nuclear	26599	4.6	37	6	**−2.3**
97	Q15056	**Eukaryotic translation initiation factor 4H (eIF-4H)**	Protein translation	Cytoplasmic/perinuclear	27385	6.7	35	9	**−2.1**
98	P28161	Glutathione S-transferase Mu 2 (GSTM2−2)	Catalytic activity	Cytoplasmic	25745	6.0	31	7	
99	P25788	Proteasome subunit α type 3 (Proteasome component C8	Multicatalytic proteinase complex	Cytoplasmic and nuclear	28433	5.2	32	11	
100	P30048	Thioredoxin-dependent peroxide reductase, mitochondrial precursor (Peroxiredoxin 3)	Redox regulation	Mitochondrial	27693	7.7	53	15	
101	P78417	Glutathione transferase omega 1 (GSTO 1−1)	Redox regulation	Cytoplasmic	27566	6.2	46	15	
102	P30041	Peroxiredoxin 6 (antioxidant protein 2)	Redox regulation	Cytoplasmic, lysosomal	25035	6.0	67	23	
103	P29354	Growth factor receptor-bound	Chaperone		25207	5.9	46	15	
104	P00938	**Triosephosphate isomerase (TIM)**	Catalytic activity		26670	6.4	50	10	**2.5**
105	P30041	**Antioxidant protein 2 (1-Cys peroxiredoxin) (Acidic calcium-independent phospholipase A2)**	Redox regulation	Cytoplasmic lysosomal	24904	6.0	69	16	**2.1**
106	P18669	Phosphoglycerate mutase 1	Catalytic activity		28804	6.7	66	25	

Table 1. (Continued)

spot	accession no.*	protein name	functions	localization	Mr theor. (Da)	pI theor.	sequence coverage (%)	peptide match	normalized delta volum[b]
107	P49914	5-formyltetrahydrofolate cyclo-ligase (MTHFS)	Catalytic activity	Cytoplasmic	23256	7.7	51	8	
108	P26583	High mobility group protein 2 (HMG-2)	Binds preferentially single-stranded DNA	Nuclear	24034	7.6	58	20	
109	P00338	**L-lactate dehydrogenase A chain (LDH-A) (LDH muscle subunit) (LDH-M)**	Catalytic activity	Cytoplasmic	36689	8.4	65	25	**3.4**
110	P27695	DNA-(apurinic or apyrimidinic site) lyase (AP endonuclease 1) (APEX nuclease) (APEN)	Repairs oxidative DNA damages	Nuclear	35555	8.3	63	18	
111	P04406	Glyceraldehyde 3-phosphate dehydrogenase, liver (GAPDH)	Catalytic activity glycolysis	Cytoplasmic	36054	8.6	63	29	
112	P40926	Malate dehydrogenase, mitochondrial precursor	Catalytic activity	Mitochondrial	35532	8.9	71	23	
113	P22626	**Heterogeneous nuclear ribonucleoproteins A2/B1 (hnRNP A2/hnRNP B1)**	RNA processing	Nuclear	37430	9.0	50	21	
114							41	19	**3.2**
115	P09651	**Heterogeneous nuclear ribonucleoprotein A1**	RNA transport	Nuclear	38846	9.3	52	22	
116							34	13	**2.4**
117	Q06830	**Peroxiredoxin 1 (Thioredoxin peroxidase 2)**	Redox regulation	Cytoplasmic	22111	8.3	81	26	**3.2**
118	P26583	High mobility group protein 2 (HMG-2)	Binds preferentially single-stranded DNA	Nuclear	24034	7.6	58	20	
119	O14818	**Proteasome subunit α type 7**	Catalytic proteinase	Cytoplasmic/ nuclear	27886	8.6	78	22	**2.6**
120	Q00688	FK506-binding protein 3 (Peptidyl-prolyl cis–trans isomerase) (PPIase) (Rotamase)	Receptors	Nuclear	25177	9.3	57	18	

[a] Accession numbers were derived from Swiss-Prot/TrEMBL database. [b] Normalized δ volume between −2.0 and 2.0. [c] In bold are listed proteins spots whose expression changes with ceramide treatment.

response to ceramide. Among them, HSP 90β is known to interact and stabilize several oncogenic protein kinases.[20]

The expression of three cytoskeletal components (tubulin β-5 chain, actin, tropomyosin α-3 chain) was found to be regulated during ceramide stimulation, suggesting a rearrangement of the cytoskeleton. In our study, the expression of tubulin-β-5 was up-regulated. The microtubules provide structural support for a cell and play an important role in cell motility, mitosis and meiosis and are also important in maintaining cell viability.[21] Rho GDP-dissociation inhibitor is an actin-related protein which regulate actin-driven assembly and is essential for the reorganization of actin filaments as a cellular response to various stimuli. In this study, Rho GDP-dissociation inhibitor is upregulated with C6-ceramide.

To confirm some of the changes in protein expression after ceramide treatment, we performed Western Blot (WB) analysis for five differentially expressed proteins (VCAM-1, Annexin V, caspase −8 and −10 and PCNA). As can be seen in Figure 2, the levels of VCAM-1 and annexin V increased as well as the cleaved form of caspase −8 and −10 in HCT116 treated with C6-ceramide. These results confirm these obtained by 2-DE. Proliferating cell nuclear antigen protein (PCNA) was found to be regulated by C6-ceramide. This protein is a component of the replication and DNA repair machinery and a known marker of cellular proliferation.[19] By 2D-gel and Western Blot (Figure 2D), we found that PCNA levels decreased with ceramide stimulation of cells, which correlates well with the nonproliferating state of these cells.

The morphological apoptotic changes induced by ceramide, such as nuclear condensation and fragmentation without a membrane rupture, were measured under light microscope after double staining with DAPI and propidium iodide. As can be seen in Figure 3, cells treated with ceramide show an apoptotic morphology (nuclear and cytoplasmic condensation, nuclear fragmentation, membrane blebbing, perinuclear chromatin condensation, and apoptotic body formation). This is in accordance with 2-DE and WB results in which we obtained an increase level of several proteins involved in apoptotic processes.

Discussion

Sphingolipids are bioactive lipids that have grasped many scientist interest since ceramide, the major breakdown product of sphingolipids, were affirmed as important lipid second messengers.[1,2] Ceramide have been shown to be released following stimulation of cells with agonists such as TNF-α, interferon-γ, interleukin-1β or chemotherapeutic agents. Furthermore, cell-permeable ceramide mimicks the actions of those agonists and exhibits antiproliferative effects and apoptosis in various cancers cell lines.[8,9] One of the most clearly illustrated target of ceramides is cell death. Interestingly, ceramides induce not only apoptosis but also caspase-independent and/or nonapoptotic cell death depending on the cell type. Recent data demonstrate that ceramides play an important role in one or several stages of apoptosis. Nevertheless, the mechanism by which ceramides mediate apoptosis has not yet been fully addressed. For exemple, it is still unknown whether ceramides are essential for the initiation or for the execution of apoptosis. And it is not entirely clear, what step of the transduction pathway leading to apoptosis is influenced or dependent on ceramide generation. The wide range of biological effects mediated by ceramides depends on many parameters such as the cell type, the nature of cell

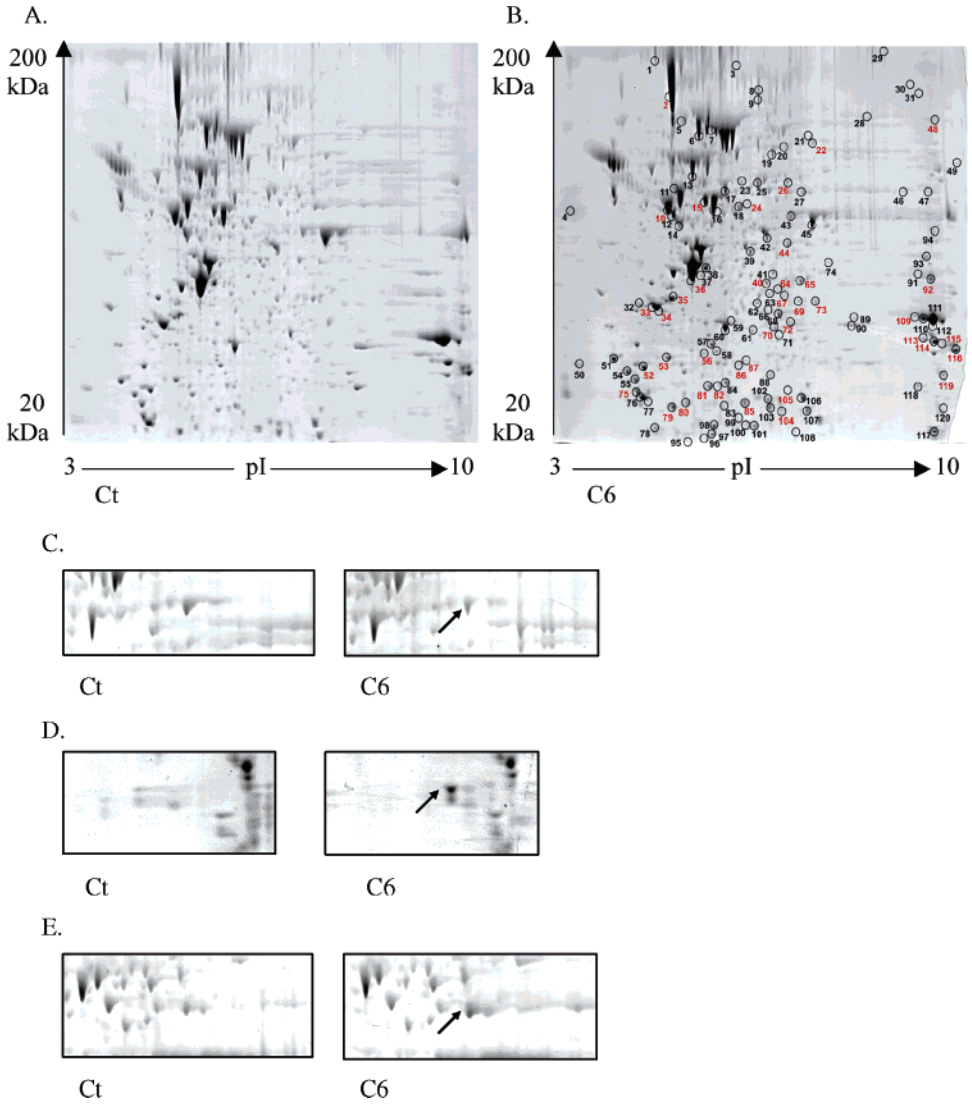

Figure 1. Representative Coomassie blue-stained 2-DE gels loaded with untreated (A) and treated with ceramide (B) HCT116 cell extracts. First dimension: IPG 3−10, 180 mm; second dimension: Duracryl 10% (255 × 205 × 1.5 mm). Among 1000 separated spots, 120 annotated spots were identified by MALDI-TOF−MS; among them 43 (annotated in red) were found to be differentially expressed Figure 1 C, D and E represented respectively close-up image of spot 22 (stress induced phosphoprotein), spot 119 (proteasome subunit α type 1) and spot 26 (caspase 10) in untreated cell extract (Ct) and in ceramide treated cell extract (C6).

receptors expressed and their concentration, suggesting the existence of multiple downstream targets activated through distinct intracellular pathways.

In this report, we applied 2-DE gel electrophoresis and the identification of proteins by mass spectrometry to the analysis of the proteome of human colon carcinoma cells (HCT116 cells). In our knowledge, this is the first 2-DE protein map of HCT116 cells. This map provide a valid basis for identifying possible differences in protein profiles of those cells in response to C6-ceramide or other stimulations. By this technique, we identified 43 proteins whose expression varied with ceramide treatment.

Stimulation of the HCT116 cells with C6-ceramide results in the induction of some proteins involved in mRNA processing, translation, replication, mobility and apoptosis. Regulation of several of these proteins was confirmed by several experimental approaches, including 2-DE gel electrophoresis, Western blotting and fluorescence microscopy, and allowed us to propose new concepts regarding ceramide pathway.

On the basis of our results, it appeared that HCT116 cells have multiple defense systems against those reactive oxygen species (ROS) such as peroxiredoxin, antioxidant protein 2 (1-Cys peroxiredoxin), glutathione synthetase and coproporphyrinogen III oxidase which are associated with various biological processes, such as the detoxification of oxidants, cell proliferation, cell differentiation and gene expression.[22] Interestingly, a redox protein, peroxiredoxin I, was found to be up-regulated upon C6-ceramide treatment. It has been previously shown that peroxiredoxin I possesses a peroxidase activity and relies on thioredoxin as a source of reducing equivalents for the reduction of the oxidant such as hydrogen peroxide.[23] Peroxiredoxins (Prxs) are important players in peroxide detoxification of the cells. Recently, a range of other cellular roles have also been attributed to mammalian peroxiredoxin family members, including the modulation of cytokine-induced hydrogen peroxide levels, which have been shown to mediate signaling cascades leading to cell proliferation, differentiation and apoptosis. This

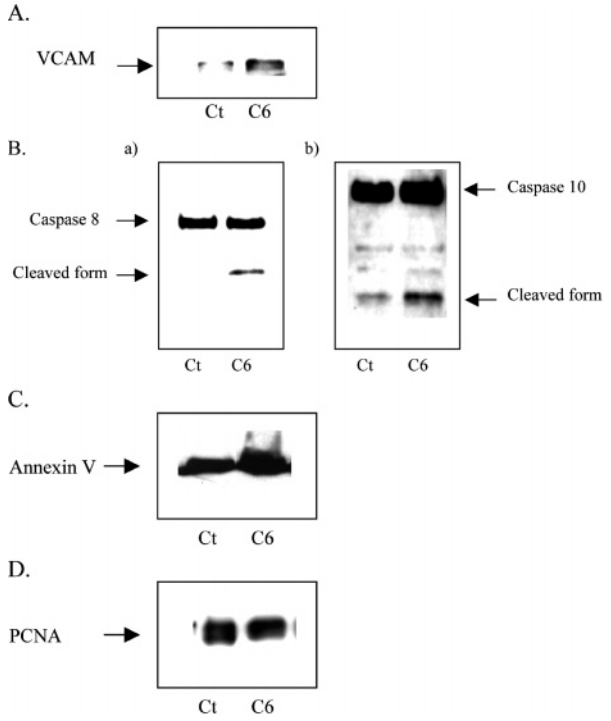

Figure 2. Validation of the 2-D gel electrophoresis data by Western blot with HCT116 treated or not with C6-ceramide during 6h. HCT116 cells were untreated (Ct), or treated for 6 h with C6-ceramide (50 μM) (C6). 20 μg of total cell lysates were separated on SDS−PAGE gel, and immunoblotting was performed with an anti-VCAM-1 (A), anti-caspase-8 and 10 (B), anti-AnnexinV (C) and anti-PCNA (D) antibodies.

diversity is reflected in slight evolutionary modifications in sequence and structure, built around a common peroxidatic active site.

When overexpressed (this is the case here), Prx enzymes reduced the intracellular level of H_2O_2 produced in stressed cells. After ceramide stimulation, cells are stressed and produced H_2O_2. Then, we believe that Prxs are overexpressed in order to detoxify the cytoplasm (cf spot 105 and 117).

RNA-interacting proteins were found to be one of the major class of proteins regulated during ceramide stimulation. This suggest that post-transcriptional control of gene expression might play a central role in ceramide pathway.

Our proteomic approach revealed an other group of proteins, namely Rho GDI 1, actin, tropomyosin and HSP 27, which are modulated by C6-ceramide and are involved in smooth muscle contraction. Rho regulates the cyskeletal system, particularly actin-dependent functions, such as cell mobility, formation of stress fibers and focal adhesions, and smooth muscle contraction. Wang and Bitar have shown that Rho plays an important role in the signal transduction modulating rabbit colon smooth muscle contractions, on stimulation by agonists such as endothelin-1 and C2-ceramide.[26] In an other study, they also propose a model in which HSP27 is involved in sustained smooth muscle contraction and modulates the interaction of actin, myosin, tropomyosin and caldesmon.[27] Another paper from Hanna et al. showed that C2-ceramide stimulate cytoskeletal changes through Ras and PI 3-K and induces stress fiber formation in Rat2 fibroblasts.[28]

PCNA is the δ subunit of DNA polymerase and is synthesized in early G1 phase and maximally expressed during S phase.

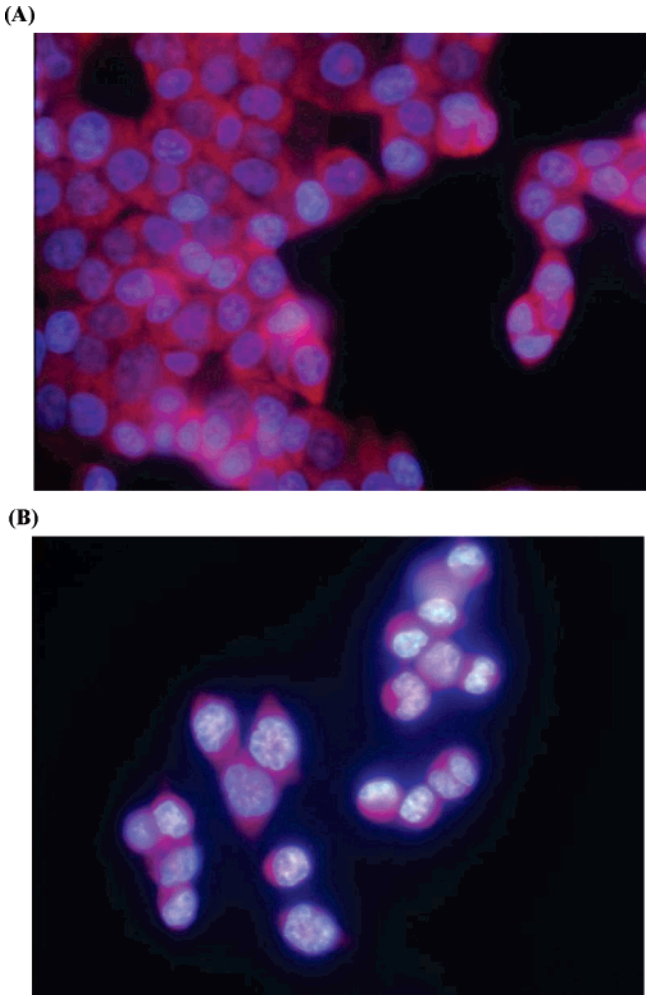

Figure 3. Cells morphology changes after ceramide treatment, HCT116 cells were untreated (A) or treated for 16 h with C6-ceramide (50 μM)(B), then doubly stained with DAPI and propidium iodide and finally observed by fluorescent microscopy.

Suppression of the expression of PCNA was shown to cause cell cycle arrest at the G1/S phase boundary. Our 2-DE and WB results demonstrated that the PCNA expression was downregulated in HCT116 cells after exposure to C6-ceramide. This result is supported by a previous study in HCT116 cells which showned a double block in G1 and G2, thus emptying the S phase after C6-ceramide stimulation. These findings are also consistent with another report showing that the expression of PCNA in ovarian cultured granulosa cells was downregulated by C6-ceramide.[29]

We also confirmed by 2-DE that ceramides, besides inhibiting proliferation, are able to induce apoptosis in HCT116 cells. We examined the effects of C6-ceramide on apoptotic cell death by means of differential 2-DE, but also by WB and by morphological evaluation. The increase of caspase-8 and -10 was observed by 2-DE and confirmed by WB after 6h of C6-ceramide treatment. In addition, drastic morphological and biochemical changes were accompanied by the cell death. A double staining with DAPI and propidium iodide showed nuclear condensation and fragmentation. All these results are consistent well with a previous study where we showed that apoptosis was associated with the induction of NF-κB DNA-binding, caspase-3 activation and poly (ADP-ribose) polymerase

(PARP) degradation, indicating that apoptosis occurs through the caspase cascade.[12]

Moreover, heat shock proteins (HSP27, HSP90, and HSP70/HSP90 organizing protein) appeared to be down-regulated by C6-ceramide. Garrido et al. described that the overexpression of heat shock 27 kDa protein in REG cells was associated with an increased tumorigenecity and with a substantial decrease of in vivo tumor cell apoptosis.[24] In our experiments, the exogeneous C6-ceramide is responsible for a decrease of heat shock proteins in HCT116 cells and is also correlated with an increase in apoptosis.

Conclusions

In the present study, 2-DE coupled with MALDI-TOF−MS allowed the reliable separation and identification of 120 proteins of HCT-116 cell line. Bioinformatic analysis revealed differential expression of cytoskeleton components, molecular chaperons, regulators of protein folding and stability, and components of RNA-processing pathways.

Taken together, our results indicated also that several proteins implied in apoptosis and growth arrest are modulated in response to ceramide. Our proteomic approach will contribute to elucidate complex characteristics of protein networks related to ceramide pathways covering various cell functions, thus may be providing new drug targets.

Acknowledgment. M.F. and M.-P.M. are Senior Research Assistants at the National Fund for Scientific Research (FNRS, Belgium). J.P. is Research Director at FNRS. We also thank the "Centre Anti-Cancéreux" (Liège, Belgium) and the National Fund for Scientific research (FNRS) for their financial support. The Proteomics facility used in this study was funded by the European Community (FEDER), the Région Nord-Pas de Calais (France), the CNRS, the Génopole of Lille and the Université des Sciences et Technologies de Lille.

References

(1) Okazaki, T.; Bell, R. M.; Hannun, Y. A. *J. Biol. Chem.* **1989**, *264*, 19076−19080.
(2) Senchenkov, A.; Litvak, D. A.; Cabot, M. C. *J. Natl. Cancer Inst.* **2001**, *93*, 347−357.
(3) Gamard, C. J.; Dbaibo, G. S.; Lui, B.; Obeid, L.; Hannun Y. *J. Biol. Chem*. **1997**, *272*, 16474−16481.
(4) Obeid, L. M.; Hannun, Y. A. *J. Cell. Biochem.* **1995**, *58*, 191−198.
(5) Verheij, M.; Bose, R.; Lin, X. H.; Yao, B.; Jarvis, W. D.; Grant, S.; Birrer, M. J.; Szabo, E.; Zon, Li; Kyriakis, J. M.; Haimovitz, F. A.; Fuks, Z.; Kolesnick, R. N. *Nature* **1996**, *380*, 75−79.
(6) Chen, C. C.; Sun, Y. T.; Chen, J. J.; Chang, Y. J. *Mol. Pharmacol.* **2001**, *59*, 493−500.
(7) Gouaze, V.; Mirault, M. E.; Carpentier, S.; Salvayre, R.; Levade, T.; Andrieu-Aradie, N. *Mol. Pharmacol.* **2001**, *60*, 488−496.
(8) Okazaki, T.; Bell, R. M.; Hannun, Y. A. *J. Biol. Chem.* **1989**, *264*, 19076−19080.
(9) Obeid, L. M.; Linardic, C. M.; Karolak, L. A.; Hannun, Y. A. *Science* **1993**, *259*, 1769−1771.
(10) Bjellqvist, B.; Ek, K.; Righetti, P. G.; Gianazza, E.; Görg, A.; Westermeier, R.; Postel, W. *J. Biochem. Biophys. Methods* **1982**, *6*, 317−339.
(11) Neuhoff, V.; Arold, N.; Taube, D.; Ehrhardt, W. *Electrophoresis* **1988**, *9*, 255−262.
(12) Fillet, M.; Bentires-Alj, M.; Deregowski, V.; Greimers, R.; Gielen, J.; Piette, J.; Bours, V.; Merville, M. P. *Biochem. Pharm.* **2003**, *65*, 1633−1642.
(13) Casella, J. F.; Torres, M. A. *J. Biol. Chem.* **1994**, *269*, 6992−6998.
(14) Mehta, D.; Rahman, A.; Malik, AB. *J. Biol. Chem.* **2001**, *276*, 22614−22620.
(15) Degryse, B.; Bonaldi, T.; Scaffidi, P.; Muller, S.; Resnati, M.; Sanvito, F.; Arrigoni, G.; Bianchi, ME. *J. Cell. Biol.* **2001**, *152*, 1197−1206.
(16) Rommelaere, H.; De Neve, M.; Neirynck, K.; Peelaers, D.; Waterschoot, D.; Goethals, M.; Fraeyman, N.; Vandekerckhove, J.; Ampe, C. *J. Biol. Chem.* **2001**, *276*, 41023−41028.
(17) Tzivion, G.; Avruch, J. *J. Biol. Chem.* **2002**, *277*, 3061−3064.
(18) Vercoutter-Edouart, A. S.; Lemoine, J.; Le Bourhis, X.; Louis, H.; Boilly, B.; Nurcombe, V.; Revillion, F.; Peyrat, J. P.; Hondermarck, H. *Cancer Res.* **2001**, *61* (1), 76−80.
(19) Kelman, Z.; Wait, R.; Rawlinson, L.; Clark A. R.; Saklatvala J. *Oncogene* **1997**, *14*, 629−640.
(20) Mendez, F.; Sandigursky, M.; Franklin, W. A.; Kenny, M. K.; Kureekattil, R.; Bases, R. *Radiat. Res.* **2000**, *153*, 186−195.
(21) Porter, L. A.; Lee, J. M. *Exp. Cell Res.* **2001**, *270*, 151−158.
(22) Fujii, J.; Ikeda, Y. *Redox. Rep.* **2002**, *7*, 123−130.
(23) Kang, S. W.; Chae, H. Z.; Seo, M. S.; Kim, K.; Baines, I. C.; Rhee, SG. *J. Biol. Chem*. **1998**, *273*, 6297−6302.
(24) Garrido, C.; Fromentin, A.; Bonnotte, B.; Favre, N.; Moutet, M.; Arrigo, A. P.; Mehlen, P.; Solary, E. *Cancer Res.* **1998**, *58*, 5495−5499.
(25) Yang, C.; Carrier, F. *J. Biol. Chem.* **2001**, *276*, 47277−47284.
(26) Wang, P.; Bitar, K. N. *Am. J. Physiol.* **1998**, *275*, 1454−1462.
(27) Ibitayo, A. I.; Sladick, J.; Tuteja, S.; Louis-Jacques, O.; Yamada, H.; Groblewski, G.; Welsh, M.; Bitar, K. N. *Am. J. Physiol*. **1999**, *277*, 445−454.
(28) Hanna, A. N.; Berthiaume, L. G.; Kikuchi, Y.; Begg, D.; Bourgoin, S.; Brindley, D. N. *Mol. Biol. Cell.* **2001**, *12*, 3618−3630.
(29) Kim, J. H.; Han, J. S.; Yoon, Y. D. *Tissue Cell.* **1999**, *31*, 531−539.

PR050006T